Time-Delay Interferometry for Space-based Gravitational Wave Searches

J. W. Armstrong, F. B. Estabrook, and Massimo Tinto

Jet Propulsion Laboratory, California Institute of Technology, Pasadena, CA 91109

Received _____; accepted _____

submitted to the Astrophysical Journal

ABSTRACT

Ground-based, equal-arm-length laser interferometers are being built to measure high-frequency astrophysical gravitational waves. Because of the arm-length equality, laser light experiences the same delay in each arm and thus phase or frequency noise from the laser itself precisely cancels at the photodetector. This laser noise cancellation is crucial. Raw laser noise is orders of magnitude larger than other noises and the desired sensitivity to gravitational waves cannot be achieved without very precise cancellation.

Laser interferometers in space, e.g. the proposed three-spacecraft LISA detector, will have much longer arm lengths and will be sensitive to much lower frequency gravitational radiation. In contrast with ground-based interferometers, it is impossible to maintain equal distances between spacecraft pairs; thus laser noise cannot be cancelled by direct differencing of the beams. We analyze here an unequal-arm three-spacecraft gravitational wave detector in which each spacecraft has one free-running laser used both as a transmitter (to send to the other two spacecraft) and as a local oscillator (to monitor the frequencies of beams received from the other two spacecraft). This produces six data streams, two received time series generated at each of the three spacecraft. We describe the apparatus in terms of Doppler transfer functions of signals and noises on these one-way transits between pairs of test masses. Accounting for time-delays of the laser light and gravitational waves propagating through the apparatus, we discuss several simple and potentially useful combinations of the six data streams, each of which exactly cancels the noise from *all three* lasers while retaining the gravitational wave signal. Three of these combinations are equivalent to unequal-arm interferometers, previously analyzed by Tinto & Armstrong 1999. The other combinations are new and may provide design

and operational advantages for space-based detectors. Since at most three laser-noise-free data streams can be independent, we provide equations relating the combinations reported here. We give the response functions of these laser-noise-canceling data combinations for both a gravity wave signal and for the remaining non-cancelled noise sources. Finally, using spacecraft separations and noise spectra appropriate for the LISA mission, we calculate the expected gravitational wave sensitivities for each laser-noise-canceling data combination.

Subject headings:

1. INTRODUCTION

The direct measurement of gravitational radiation will yield otherwise unobtainable information about massive astrophysical sources. High-sensitivity detection methods include resonant bars, Doppler tracking of spacecraft, and broadband laser interferometers (Thorne 1987). Ground-based interferometric gravitational wave (GW) detectors (e.g. Abramovici *et al.* 1992, Caron *et al.* 1997, Kawabe *et al.* 1997, Lück *et al.* 1997) will search for high-frequency ($\sim$10 – 1000 Hz) gravitational waves. Space-borne interferometers, such as LISA (Bender *et al.* 1998), have been proposed to detect and study *low*-frequency ($\sim$0.1 – 100 mHz) waves.

Earth-based interferometers operate in the long-wavelength limit, or LWL (arm lengths $<<$ gravitational wavelength $\sim c/f_0$, where f_0 is a characteristic frequency of the GW). By contrast, the Doppler tracking technique and space-borne interferometers involve much longer arm-lengths and, over much of the low-frequency band where they are sensitive, are *not* in the LWL. When the physical scale of a free mass optical interferometer intended to detect gravitational waves is comparable to or larger than the GW wavelength, time delays in the response of the instrument to the waves, and travel times along beams in the instrument, must be allowed for in the theory of the detector response used for data interpretation. It is convenient to formulate the instrumental responses in terms of observed differential frequency shifts – for short, Doppler shifts – rather than in terms of phase shifts usually used in interferometry, although of course these data, as functions of time, are interconvertible.

Time-of-flight delays also are important in space interferometry when, inevitably, path lengths cannot be made equal. In this case *in situ* homodyne detection – direct interference of beams – will not cancel laser frequency noise to the threshold of secondary fluctuations. In order to achieve laser noise cancellation, the time-varying Doppler data must be recorded

and post-processed to allow for arm-length differences. The data streams will have temporal structure, which can be described as due to many-pulse responses to δ-function excitations, depending on time-of-flight delays in the response functions of the instrumental Doppler noises and in the response to incident plane-parallel gravitational waves. Previous papers in this spirit have dealt with the Doppler response to gravitational waves of a coherent microwave link between the Earth and a distant spacecraft (three-pulse GW response) (Estabrook & Wahlquist 1975), with the response of an equi-arm Michelson interferometer (four-pulse GW response) (Estabrook 1985), and with unequal arm interferometers (eight-pulse GW response) (Tinto & Armstrong 1999).

The LISA gravitational wave observatory will use three spacecraft orbiting the sun. Each spacecraft would be equipped with a laser sending beams to the other two ($\sim$0.03 AU away) while simultaneously detecting (using the same laser) the frequencies of the laser beams received from the other two. We assume in the following successful prior removal of any first-order Doppler beat notes due to relative motions, giving six residual Doppler time series as the raw data of a *stationary* time delay space interferometer. We suggest that it is best to think of LISA not as constituting one or more conventional Michelson interferometers, but rather, in a symmetrical way, to consider a closed array of six one-arm delay lines between the test masses. In this way we can produce new data combinations which cancel laser noises, and compute achievable sensitivities of these combinations in terms of the separate and relatively simple GW and instrumental noise one-arm responses (cf. Tinto 1996, Tinto 1998).

In Section 2 we summarize the one-arm Doppler transfer functions of an optical beam between two spacecraft due to various excitations: incident transverse traceless gravitational waves, frequency fluctuations of the lasers used in transmission and reception, fluctuations due to non-inertial motions of the spacecraft, and shot noise introduced at the readout.

The dominant noise, by many orders of magnitude, is frequency fluctuations in the lasers. These noises must be very precisely removed from the data to achieve GW sensitivity at levels set by the much lower remaining Doppler noise sources.

In Section 3 we show how all three laser noises can be eliminated by suitably delaying and linearly combining the six LISA data streams. A three parameter manifold of high-precision data streams suitable for gravitational wave analysis results. A symmetrical basis that elegantly spans the space of laser-noise-free data is found, combinations of the six data streams that we denote α, β, and γ. Each of these combines the raw data with copies of it delayed by one or two single-arm transit times. α, β, and γ each has a six-pulse response to incident gravitational waves; that is, a passing delta function of metric distortion will be seen six times in each of these streams.

A six-pulse laser-noise-free combination denoted ζ, for which each raw data set need only be delayed by *single* arm transit times, is also introduced, and its relation to α, β, and γ given. The response of ζ to gravitational waves becomes of higher order, however, in the special case where the spacecraft separations are equal; this may be an argument for preferring an isosceles or scalene triangular configuration of spacecraft.

We then express the recently-discovered laser-noise-free combinations for each of the three possible unequal-arm interferometers in the LISA array (Tinto & Armstrong 1999) in terms of α, β, and γ with further transit time delays. We call these X, Y, and Z; they have eight-pulse responses to gravitational radiation. One of these interferometric data combinations would still be available if the links between one pair of spacecraft were lost. We show how the unequal-arm interferometer data combinations X, Y, and Z can be constructed by combining one-way data streams; the present LISA design equivalently produces them using optical transponders.

Other eight-pulse combinations, denoted P, Q and R, each of which requires data taken

at only two of the spacecraft, are also presented.

In Section 4 we compute the response to sinusoidal gravitational radiation of each of the laser-noise-canceling linear combinations (α, β, γ, ζ, X, Y, Z, P, Q, R) as a function of frequency, suitably averaging over source directions and wave polarization states. We also compute the aggregate noise spectrum for each of these data combinations, taking into account appropriate transfer functions. The ratio of the rms noise to the rms signal response then gives the sensitivity of each data combination to gravitational waves as a function of Fourier frequency. The spectral region where these ratios are minimum sets the observational passband and threshold sensitivity for a space-based gravitational wave search. These plots for X, Y, Z can directly be compared to previous feasibility calculations for LISA, which assumed an equal-arm Michelson interferometer configuration.

2. DOPPLER RESPONSE FUNCTIONS

2.1. Notation

Figure 1 shows the geometry in the plane of the three-spacecraft LISA detector. The spacecraft are labeled 1, 2, 3 and are equidistant (distance = l) from point O. Relative to O, the spacecraft are located by the coplanar unit vectors $\hat{p}_1$, $\hat{p}_2$, $\hat{p}_3$. As indicated in Figure 1, the lengths between pairs of spacecraft are L_1, L_2, L_3, with L_i being opposite spacecraft i. Unit vectors along the lines connecting spacecraft pairs are $\hat{n}_1$, $\hat{n}_2$, $\hat{n}_3$, oriented such that $\hat{n}_1$ has its foot at spacecraft 3 and its arrow pointing at spacecraft 2, $\hat{n}_2$ has its foot at spacecraft 1 and its arrow pointing toward spacecraft 3, and $\hat{n}_3$ has its foot at spacecraft 2 and its arrow pointing toward spacecraft 1. Thus $L_1\hat{n}_1 + L_2\hat{n}_2 + L_3\hat{n}_3 = 0$. This terminology allows us to cyclically permute indices in subsequent equations, and so in fact only 1/3 as many equations need be written explicitly.

Each spacecraft has a laser which is used both to transmit a narrow-band beam to the other two spacecraft and (as a local oscillator) to produce a Doppler time series from the beams received from the other two spacecraft. Thus there are six Doppler time series produced, involving reception of two beams at each of three spacecraft. We denote these six Doppler data streams, each divided by the nominal center frequency of the lasers, ν_0, as y_{ij}, with i not equal to j. The subscript convention is that, e.g., y_{31} is the (fractional or normalized – we omit the qualifier in the rest of this paper) Doppler series derived from reception at spacecraft 1 with transmission from spacecraft 2. Similarly, y_{21} is the Doppler derived from reception at spacecraft 1 with transmission at spacecraft 3. The other four Doppler time series are obtained by cyclic permutation of the indices, above: $1 \rightarrow 2 \rightarrow 3 \rightarrow 1$. We will also use a useful notation for the data streams further delayed in post-processing: $y_{31,2} = y_{31}(t - L_2)$, $y_{31,23} = y_{31}(t - L_2 - L_3) = y_{31,32}$, etc. (we have here taken c = 1).

2.2. Signal and Noise Response Functions

Any gravitational wave signal and the various noises enter the Doppler observations y_{ij} via transfer functions. In this subsection we summarize the response functions for a general signal and the principal noise processes.

Signal Transfer Function

The response of the one-way Doppler time series y_{ij} excited by a transverse, traceless plane gravitational wave having unit wavevector $\hat{k}$ is, in the above notation, (Wahlquist 1987):

$$y_{31}^{gw}(t) = \left[1 + \frac{l}{L_3}(\mu_1 - \mu_2)\right] (\Psi_3(t - \mu_2 l - L_3) - \Psi_3(t - \mu_1 l)) \qquad (1)$$

$$y_{21}^{gw}(t) = \left[1 - \frac{l}{L_2}(\mu_3 - \mu_1)\right] (\Psi_2(t - \mu_3 l - L_2) - \Psi_2(t - \mu_1 l)) \quad (2)$$

where $\mu_i = \hat{k} \cdot \hat{p}_i$, and Ψ_i is

$$\Psi_i(t) = \frac{1}{2} \frac{\hat{n}_i \cdot \mathbf{h}(t) \cdot \hat{n}_i}{1 - (\hat{k} \cdot \hat{n}_i)^2} \quad (3)$$

and where $\mathbf{h}(t)$ is the first order spatial metric perturbation at point O. Note that $L_1 \hat{k} \cdot \hat{n}_1 = l(\mu_2 - \mu_3)$, and so forth by cyclic permutation of the indices. The gravitational wave $\mathbf{h}(t)$ is $[h_+(t)\ \mathbf{e}_+ + h_\times(t)\ \mathbf{e}_\times]$, where the 3-tensors $\mathbf{e}_+$ and $\mathbf{e}_\times$ are transverse to $\hat{k}$ and traceless. With respect to an orthonormal propagation frame $(\hat{i}, \hat{j}, \hat{k})$ their components are:

$$\mathbf{e}_+ = \begin{pmatrix} 1 & 0 & 0 \\ 0 & -1 & 0 \\ 0 & 0 & 0 \end{pmatrix}, \mathbf{e}_\times = \begin{pmatrix} 0 & 1 & 0 \\ 1 & 0 & 0 \\ 0 & 0 & 0 \end{pmatrix} \quad (4a)$$

Noise Transfer Functions

Fluctuations in the laser frequency at each of the spacecraft are the main noise source and must be cancelled by 7 to 10 orders of magnitude to reach LISA's desired sensitivity. We denote frequency fluctuation noise of the laser aboard the i-th spacecraft divided by the nominal frequency ν_0 by C_i(t). That is, the instantaneous frequency is $\nu_i(t) = \nu_0(1 + C_i(t))$.

The laser noise of the *receiving* spacecraft enters the Doppler data immediately at the time of reception, while the laser noise of the *transmitting* spacecraft enters at a one-way delay time earlier. The responses in the six Doppler time series to laser noise are thus:

$$y_{31}^{laser} = C_2(t - L_3) - C_1(t) \tag{5}$$

$$y_{21}^{laser} = C_3(t - L_2) - C_1(t) \tag{6}$$

with the laser noise contributions to the other four Doppler time series obtained by cyclic permutation of the indices.

Shot noise, n_{ij}^s(t), enters each Doppler time series in the reception process at spacecraft j. It is white phase noise so its effect on the derivative of phase, the Doppler time series, has a power spectral density proportional to f^2 where f is the Fourier frequency. Its effect is immediate at the time of reception, so that the responses of the Doppler observables are:

$$y_{31}^{shot} = n_{31}^s(t) \tag{7}$$

$$y_{21}^{shot} = n_{21}^s(t) \tag{8}$$

Imperfections in the ability of each spacecraft strictly to maintain free-fall are called, in the LISA context, inertial sensor or acceleration noise (Bender *et al.* 1998); this noise enters most strongly at low frequencies. The integral of these stochastic accelerations gives velocity noises which affect the Doppler. From Figure 1, if spurious, isotropic accelerations at the three spacecraft produce random velocity errors $\vec{v}_i(t)$, i = 1, 2, 3, then the response in the Doppler observables will depend on the senses of the laser beams and involve propagation delays:

$$y_{31}^{accel}(t) = \hat{n}_3 \cdot \vec{v}_2(t - L_3) - \hat{n}_3 \cdot \vec{v}_1(t) \quad (9)$$

$$y_{21}^{accel}(t) = -\hat{n}_2 \cdot \vec{v}_3(t - L_2) + \hat{n}_2 \cdot \vec{v}_1(t) \quad (10)$$

(c = 1) with the other four Doppler time series obtained, as usual, by cyclic permutation of the indices.

In the following we model the six time series as linear sums of the above signal and noises:

$$y_{ij}(t) = y_{ij}^{gw}(t) + y_{ij}^{laser}(t) + y_{ij}^{shot}(t) + y_{ij}^{accel}(t) \quad (11)$$

For the sensitivity calculations of Section 4, we use detector dimensions and noise spectral levels appropriate for LISA.

3. LINEAR DATA COMBINATIONS WHICH ELIMINATE ALL LASER NOISES

With independent lasers on two spacecraft laser-noise cancellation can be achieved at selected Fourier frequencies (Tinto 1998); with three spacecraft the increased number of Doppler signals allows closure and removal of laser noises at *all* frequencies. Indeed, given the six experimental data streams $y_{ij}(t)$, one can solve the linear first difference equations (11) to find combinations which eliminate one or more of the noises. Since for LISA frequency fluctuations in the three lasers, y_{ij}^{laser}, dominate, we seek to cancel these noises.

In this section we present what appears to be the ten simplest linear combinations which cancel the laser noises from all of the spacecraft. Since only three such combinations can be independent, we accordingly note seven relations between them. We assume throughout a stationary configuration with sufficient knowledge of arm lengths and adequate clock synchronization between the three spacecraft (Tinto & Armstrong 1999).

3.1. The α, β, γ (Six-Pulse) Combinations

As can be verified by direct substitution of the laser noise contributions (equations 5, 6), three independent linear combinations of the Doppler data which do not contain *any* laser noise are:

$$\alpha = y_{21} - y_{31} + y_{13,2} - y_{12,3} + y_{32,12} - y_{23,13} \tag{12}$$

and β, γ given by cyclic permutation of the indices; explicitly:

$$\beta = y_{32} - y_{12} + y_{21,3} - y_{23,1} + y_{13,23} - y_{31,21} \tag{13}$$

$$\gamma = y_{13} - y_{23} + y_{32,1} - y_{31,2} + y_{21,31} - y_{12,32} \tag{14}$$

These linear combinations seem to us to be the simplest suitable basis for laser-noise-free data. Each has a six-pulse response to gravitational wave signals. This can be demonstrated by substituting the gravitational wave responses for the y_{ij} (equations 1, 2) into the α, β, γ expressions, above. Explicitly, for α, the gravitational wave response is:

$$
\begin{aligned}
\alpha^{gw} \;=\; & \left[1 - \frac{l}{L_2}(\mu_3 - \mu_1)\right] \left(\Psi_2(t - \mu_3 l - L_2) - \Psi_2(t - \mu_1 l)\right) \\
& - \left[1 + \frac{l}{L_3}(\mu_1 - \mu_2)\right] \left(\Psi_3(t - \mu_2 l - L_3) - \Psi_3(t - \mu_1 l)\right) \\
& + \left[1 - \frac{l}{L_1}(\mu_2 - \mu_3)\right] \left(\Psi_1(t - \mu_2 l - L_1 - L_2) - \Psi_1(t - \mu_3 l - L_2)\right) \\
& - \left[1 + \frac{l}{L_1}(\mu_2 - \mu_3)\right] \left(\Psi_1(t - \mu_3 l - L_1 - L_3) - \Psi_1(t - \mu_2 l - L_3)\right) \\
& + \left[1 - \frac{l}{L_3}(\mu_1 - \mu_2)\right] \left(\Psi_3(t - \mu_1 l - L_3 - L_1 - L_2) - \Psi_3(t - \mu_2 l - L_1 - L_2)\right) \\
& - \left[1 + \frac{l}{L_2}(\mu_3 - \mu_1)\right] \left(\Psi_2(t - \mu_1 l - L_2 - L_1 - L_3) - \Psi_2(t - \mu_3 l - L_1 - L_3)\right) \quad (15)
\end{aligned}
$$

with Ψ_i, l, μ_i, L_i given in terms of the tensor gravitational wave properties and the detector geometry as given in Section 2. A δ-function GW, $\mathbf{h}(t) = \mathbf{H}\ \delta(t)$, would produce six pulses in α, located with relative times depending on the arrival direction of the wave and the detector configuration: $\mu_1 l$, $\mu_3 l + L_2$, $\mu_2 l + L_3$, $\mu_2 l + L_1 + L_2$, $\mu_3 l + L_1 + L_3$, and $\mu_1 l + L_1 + L_2 + L_3$.

3.2. Fully Symmetric (Sagnac) Combination

A symmetric combination which also exactly cancels all laser noises is ζ, given by:

$$\zeta = y_{32,2} - y_{23,3} + y_{13,3} - y_{31,1} + y_{21,1} - y_{12,2} \quad (16)$$

which can be written in terms of α, β, and γ as:

$$\zeta - \zeta_{,123} = \alpha_{,1} - \alpha_{,23} + \beta_{,2} - \beta_{,31} + \gamma_{,3} - \gamma_{,12} \quad (17)$$

ζ has the property that each of the y_{ij} data streams enters exactly once and each is lagged by exactly one of the one-way light times. Its response to gravitational waves is:

$$\begin{aligned}
\zeta^{gw} \;=\; & \left[1-\frac{l}{L_3}(\mu_1-\mu_2)\right](\Psi_3(t-\mu_1 l-L_3-L_2)-\Psi_3(t-\mu_2 l-L_2)) \\
& -\left[1+\frac{l}{L_2}(\mu_3-\mu_1)\right](\Psi_2(t-\mu_1 l-L_2-L_3)-\Psi_2(t-\mu_3 l-L_3)) \\
& +\left[1-\frac{l}{L_1}(\mu_2-\mu_3)\right](\Psi_1(t-\mu_2 l-L_1-L_3)-\Psi_1(t-\mu_3 l-L_3)) \\
& -\left[1+\frac{l}{L_3}(\mu_1-\mu_2)\right](\Psi_3(t-\mu_2 l-L_3-L_1)-\Psi_3(t-\mu_1 l-L_1)) \\
& +\left[1-\frac{l}{L_2}(\mu_3-\mu_1)\right](\Psi_2(t-\mu_3 l-L_2-L_1)-\Psi_2(t-\mu_1 l-L_1)) \\
& -\left[1+\frac{l}{L_1}(\mu_2-\mu_3)\right](\Psi_1(t-\mu_3 l-L_1-L_2)-\Psi_1(t-\mu_2 l-L_2)) \qquad (18)
\end{aligned}$$

A δ-function GW signal would produce six pulses in ζ, located at: $\mu_1 l + L_3 + L_2$, $\mu_2 l + L_1 + L_3$, $\mu_3 l + L_1 + L_2$, $\mu_3 l + L_3$, $\mu_2 l + L_2$, and $\mu_1 l + L_1$.

3.3. Unequal-Arm-Length Interferometric Combinations

Of course α, β, and γ are not unique; they span a three-space of combinations which produce data free of laser noise. For example, there are combinations which cancel all laser noises while giving eight-pulse responses to gravitational waves:

$$X = y_{32,322} - y_{23,233} + y_{31,22} - y_{21,33} + y_{23,2} - y_{32,3} + y_{21} - y_{31} \qquad (19)$$

and Y, Z given by cyclic permutation of the indices. These can be expressed directly in terms α, β, and γ as:

$$X_{,1} = \alpha_{,32} - \beta_{,2} - \gamma_{,3} + \zeta \tag{20}$$

$$Y_{,2} = \beta_{,13} - \gamma_{,3} - \alpha_{,1} + \zeta \tag{21}$$

$$Z_{,3} = \gamma_{,21} - \alpha_{,1} - \beta_{,2} + \zeta \tag{22}$$

Note that X does not involve y_{13} and y_{12}, so it would still be available if the laser links between spacecraft 2 and 3 were lost. A similar argument applies for Y and Z. If transponders were used in spacecraft 2 and 3 to slave the frequencies generated there to the uplink frequency received from spacecraft 1, they impose the conditions $y_{32} = y_{23} = 0$ (perhaps then also adding transponder noises which we do not consider here). Then X becomes a combination of data taken only at spacecraft 1:

$$y_{32} = y_{23} = 0$$

$$X \rightarrow \Sigma \equiv y_{31,22} - y_{31} - y_{21,33} + y_{21} \tag{23}$$

This is the laser-noise-free unequal-arm interferometer time series first given in Tinto & Armstrong 1999, with its eight-pulse response to a gravitational wave signal. Evidently X in equation (19) is a *synthesized* interferometer response using one-way Doppler data from all three spacecraft.

Explicitly, for X, the gravitational wave response is:

$$X^{gw} = \left[1 - \frac{l}{L_3}(\mu_1 - \mu_2)\right] (\Psi_3(t - \mu_1 l - 2L_3 - 2L_2) - \Psi_3(t - \mu_2 l - L_3 - 2L_2))$$

$$
\begin{aligned}
&-\left[1+\frac{l}{L_2}(\mu_3-\mu_1)\right]\,(\Psi_2(t-\mu_1 l-2L_2-2L_3)-\Psi_2(t-\mu_3 l-L_2-2L_3))\\
&+\left[1+\frac{l}{L_3}(\mu_1-\mu_2)\right]\,(\Psi_3(t-\mu_2 l-L_3-2L_2)-\Psi_3(t-\mu_1 l-2L_2))\\
&-\left[1-\frac{l}{L_2}(\mu_3-\mu_1)\right]\,(\Psi_2(t-\mu_3 l-L_2-2L_3)-\Psi_2(t-\mu_1 l-2L_3))\\
&+\left[1+\frac{l}{L_2}(\mu_3-\mu_1)\right]\,(\Psi_2(t-\mu_1 l-2L_2)-\Psi_2(t-\mu_3 l-L_2))\\
&-\left[1-\frac{l}{L_3}(\mu_1-\mu_2)\right]\,(\Psi_3(t-\mu_1 l-2L_3)-\Psi_3(t-\mu_2 l-L_3))\\
&+\left[1-\frac{l}{L_2}(\mu_3-\mu_1)\right]\,(\Psi_2(t-\mu_3 l-L_2)-\Psi_2(t-\mu_1 l))\\
&-\left[1+\frac{l}{L_3}(\mu_1-\mu_2)\right]\,(\Psi_3(t-\mu_2 l-L_3)-\Psi_3(t-\mu_1 l)) \qquad (24)
\end{aligned}
$$

with Ψ_i, l, μ_i, L_i given in terms of the wave properties and detector geometry as in Section 2. A δ-function GW signal would produce eight pulses in X, at times depending on the arrival direction of the wave and the detector configuration: $\mu_1 l$, $\mu_2 l + L_3$, $\mu_3 l + L_2$, $\mu_1 l + 2L_3$, $\mu_1 l + 2L_2$, $\mu_3 l + L_2 + 2L_3$, $\mu_2 l + 2L_2 + L_3$, and $\mu_1 l + 2L_2 + 2L_3$.

3.4. Combinations With Data Taken at Two Spacecraft

Laser-noise-free combinations are not exhausted by those we discussed above. The interesting ones, of course, are not just superpositions of the three bases α, β, and γ, but should also have simple correlation structure – a low number of pulses in response to gravitational waves. The sensitivities and directional responses of all of these must eventually be investigated. To give an example consider:

$$P = y_{32,2} - y_{23,3} - y_{12,2} + y_{13,3} + y_{12,13} - y_{13,12} + y_{23,311} - y_{32,211} \qquad (25)$$

together with Q and R from cyclic permutation. P has an 8-pulse response to incident

gravitational waves, viz. pulses at times $\mu_3 l + L_3$, $\mu_2 l + L_2$, $\mu_1 l + L_2 + L_3$, $\mu_2 l + L_1 + L_3$, $\mu_3 l + L_1 + L_2$, $\mu_1 l + 2L_1 + L_2 + L_3$, $\mu_2 l + 2L_1 + L_2$, and $\mu_3 l + 2L_1 + L_3$.

In terms of the bases we have:

$$P = \zeta - \alpha_{,1} \tag{26}$$

The P, Q, R combinations could be useful in that each only involves data received at two of the spacecraft. The gravitational wave response for P is:

$$\begin{aligned}
P^{gw} \;=\; & \left[1 - \frac{l}{L_3}(\mu_1 - \mu_2)\right] (\Psi_3(t - \mu_1 l - L_3 - L_2) - \Psi_3(t - \mu_2 l - L_2)) \\
& - \left[1 + \frac{l}{L_2}(\mu_3 - \mu_1)\right] (\Psi_2(t - \mu_1 l - L_2 - L_3) - \Psi_2(t - \mu_3 l - L_3)) \\
& - \left[1 + \frac{l}{L_1}(\mu_2 - \mu_3)\right] (\Psi_1(t - \mu_3 l - L_1 - L_2) - \Psi_1(t - \mu_2 l - L_2)) \\
& + \left[1 - \frac{l}{L_1}(\mu_2 - \mu_3)\right] (\Psi_1(t - \mu_2 l - L_1 - L_3) - \Psi_1(t - \mu_3 l - L_3)) \\
& + \left[1 + \frac{l}{L_1}(\mu_2 - \mu_3)\right] (\Psi_1(t - \mu_3 l - 2L_1 - L_3) - \Psi_1(t - \mu_2 l - L_1 - L_3)) \\
& - \left[1 - \frac{l}{L_1}(\mu_2 - \mu_3)\right] (\Psi_1(t - \mu_2 l - 2L_1 - L_2) - \Psi_1(t - \mu_3 l - L_1 - L_2)) \\
& + \left[1 + \frac{l}{L_2}(\mu_3 - \mu_1)\right] (\Psi_2(t - \mu_1 l - 2L_1 - L_2 - L_3) - \Psi_2(t - \mu_3 l - 2L_1 - L_3)) \\
& - \left[1 - \frac{l}{L_3}(\mu_1 - \mu_2)\right] (\Psi_3(t - \mu_1 l - 2L_1 - L_2 - L_3) - \Psi_3(t - \mu_2 l - 2L_1 - L_2))
\end{aligned} \tag{27}$$

3.5. Long-Wavelength Limits

Although LISA will not operate exclusively in the long-wavelength limit, LWL analytical results are useful. In the LWL, the gravitational wave can be expanded in terms

of spatial derivatives, e.g.

$$\mathbf{h}(t-\mu_2 l - L_3) = \mathbf{h}(t) - (\mu_2 l + L_3)\mathbf{h}'(t) + (1/2)(\mu_2 l + L_3)^2 \mathbf{h}''(t) + ...$$

The y_{ij}^{gw} are of order $\mathbf{h}'$, while α, β, γ, ζ, X, Y, Z, P, Q, and R are of order $\mathbf{h}''$. The long wavelength expansions are

$$\begin{aligned} \alpha^{gw} \rightarrow \quad & (1/2)L_1(L_2 - L_3)\ \hat{n}_1 \cdot \mathbf{h}'' \cdot \hat{n}_1 \\ & -(1/2)L_2(L_1 + L_3)\ \hat{n}_2 \cdot \mathbf{h}'' \cdot \hat{n}_2 \\ & +(1/2)L_3(L_2 + L_1)\ \hat{n}_3 \cdot \mathbf{h}'' \cdot \hat{n}_3 \end{aligned} \tag{28}$$

$$\begin{aligned} \zeta^{gw} \rightarrow \quad & (1/2)L_1(L_3 - L_2)\ \hat{n}_1 \cdot \mathbf{h}'' \cdot \hat{n}_1 \\ & +(1/2)L_2(L_1 - L_3)\ \hat{n}_2 \cdot \mathbf{h}'' \cdot \hat{n}_2 \\ & +(1/2)L_3(L_2 - L_1)\ \hat{n}_3 \cdot \mathbf{h}'' \cdot \hat{n}_3 \end{aligned} \tag{29}$$

$$\begin{aligned} X^{gw} \rightarrow \quad & (1/2)L_1(L_2 - L_3)\ \hat{n}_1 \cdot \mathbf{h}'' \cdot \hat{n}_1 \\ & -(1/2)L_2(L_1 + 3L_3)\ \hat{n}_2 \cdot \mathbf{h}'' \cdot \hat{n}_2 \\ & +(1/2)L_3(L_1 + 3L_2)\ \hat{n}_3 \cdot \mathbf{h}'' \cdot \hat{n}_3 \end{aligned} \tag{30}$$

$$\begin{aligned} P^{gw} \rightarrow \quad & L_1(L_3 - L_2)\ \hat{n}_1 \cdot \mathbf{h}'' \cdot \hat{n}_1 \\ & +L_2 L_1\ \hat{n}_2 \cdot \mathbf{h}'' \cdot \hat{n}_2 \\ & -L_3 L_1\ \hat{n}_3 \cdot \mathbf{h}'' \cdot \hat{n}_3 \end{aligned} \tag{31}$$

with β and γ derived from α, Y and Z derived from X, and Q and R derived from P by cyclic permutation of the indices. Note that in the case of an equilateral triangle, the LWL response of ζ is nonzero beginning with $\mathbf{h}'''$.

4. GRAVITATIONAL WAVE SENSITIVITIES

In this section we compute the sensitivity to GWs, i.e. the strength of a GW required to achieve a given signal-to-noise ratio as a function of Fourier frequency across the LISA band, for each of the data combinations which cancel laser noise.

4.1. RMS Gravitational Wave Response

To calculate average sensitivity of the various laser-noise-canceling combinations of the y_{ij}, we assume an elliptically-polarized monochromatic gravitational wave incident on the three-spacecraft system: $h_+ = \mathrm{H}\ \sin\Gamma\ \sin(\omega t + \phi)$ and $h_\times = \mathrm{H}\ \cos\Gamma\ \sin\omega t$, where H characterizes the strength of the gravitational wave and (Γ, ϕ) define its polarization state. Γ and ϕ are related to coordinates on the Poincaré sphere for spin-2 waves. Let ($\hat{u}$, $\hat{v}$) be orthogonal unit vectors in the plane of the three spacecraft, with $\hat{w}$ forming a right hand system. To calculate the scalar responses Ψ_i, we express the orientations of the $\hat{n}_i$ by their angles a_i with the $\hat{u}$ axis. The orientation of the wavevector $\hat{k}$ (which is the opposite of the direction to the source) is specified by spherical angles (R, D); ; R is the angle in the plane of LISA between the projection of $\hat{k}$ into that plane and $\hat{n}_1$, while D is the angle between the projection and $\hat{k}$. Then equation (3) becomes

$$\Psi_i(t) \;=\; \left[\frac{H}{2(1-(\hat{k}\cdot\hat{n}_i)^2)}\right]\;[P_i\ cos(\omega t) + Q_i\ sin(\omega t)] \qquad (32)$$

where $P_i = \sin\Gamma \sin\phi\ (\sin^2 D \cos^2(a_i - R) - \sin^2(a_i - R))$ and $Q_i = (\sin\Gamma \cos\phi)\ (\sin^2 D \cos^2(a_i - R) - \sin^2(a_i - R)) - 2 \cos\Gamma \sin(a_i - R) \cos(a_i - R) \sin D$. We substitute this expression for Ψ_i into equations (1) and (2) to get expressions for y_{ij}^{gw}. Since the excitation is assumed sinusoidal, the (linear) responses y_{ij}^{gw} are also sinusoidal. The y_{ij}^{gw} are then used to produce expressions for GW response of the laser-noise-canceling combinations. For example, we substitute into equation (15) to get α^{gw}, into equation (18) to get ζ^{gw}, and into equation (24) to get X^{gw}.

To produce the rms gravitational wave response of each α, ζ, X, ... combination, we use a procedure similar to one used for spacecraft Doppler tracking GW sensitivity calculations (Armstrong, Estabrook, & Wahlquist 1987). We average over source directions (assumed uniformly distributed on the celestial sphere) and polarization states (assumed uniformly distributed on the Poincaré sphere for each source direction). The averaging is done via Monte Carlo computer simulation with 2500 (source position, polarization state) pairs per Fourier frequency bin and 7000 Fourier bins across the LISA band ($\sim 10^{-4}$ Hz to $\sim 10^{-1}$ Hz). The nominal LISA configuration is an almost equilateral triangle; we took $L_1 = L_2 = L_3 = 10\sqrt{3}$ light seconds in all calculations (except for the unequal arm ζ case, discussed below).

Figure 2 shows the rms spectral response of equal-arm α^{gw}, equal-arm ζ^{gw}, unequal-arm ζ^{gw}, and equal-arm X^{gw} and P^{gw} as a function of Fourier frequency. The GW response is suppressed in the LWL, since for sinusoidal waves $\mathbf{h}''(\mathbf{t})$ brings in a factor of f^2. The equal-arm rms α^{gw}, equal-arm rms X^{gw} and P^{gw}, and unequal-arm rms ζ^{gw} (see Section 3.5) show this LWL dependence. The equal-arm rms ζ^{gw} varies as f^3 (equation 29). The rms responses peak roughly when the GW period becomes comparable to the light times between spacecraft pairs, with oscillations in the response as the phasors associated with each of the GW pulses add constructively and destructively. The response at higher

frequencies remains comparable to the peak response and varies with Fourier frequency as the GW phasors in α^{gw}, ζ^{gw}, and X^{gw} add in an out of phase.

4.2. Noise Spectra

To compute the spectra of the important remaining noises for each data combination, we begin with the raw Doppler power spectra of shot and accelerations noises and multiply each of them by the square of the Fourier transform of the temporal transfer function relevant to the various laser-noise-canceling combinations. Acceleration and shot noise are assumed independent, so their spectra add to give the composite noise spectrum. Explicitly, specification for acceleration noise performance in Bender *et al.* 1998 is characterized by the spectrum $10^{-30} \times [1 + (f/3 \times 10^{-3} Hz)^2]^2 \; [f/10^{-4} Hz]^{-2/3}$ $(\mathrm{m/s^2})^2/\mathrm{Hz}$. We assume this spectrum for acceleration noise at each spacecraft along a given beam and convert to a raw spectrum of fractional frequency fluctuations, S_y^{accel}, by dividing it by $4\pi^2 f^2 c^2$, where c is the speed of light, yielding $S_y^{accel} = 2.8 \times 10^{-41} [1 + (f/3 \times 10^{-3} Hz)^2]^2 \; [f/10^{-4} Hz]^{-8/3}$ Hz^{-1}. (Note that we use physical units in this conversion; we used c = 1 elsewhere.) The shot noise spectrum used was derived from the length noise spectrum in the LISA Pre-Phase A report ($11 \times 10^{-12} m/\sqrt{Hz}$) to be, for fractional frequency fluctuations, S_y^{shot} $= 5.3 \times 10^{-38} \; (f/1Hz)^2 \; \mathrm{Hz}^{-1}$.

For example, the noise spectrum for α was computed using the above raw spectra for shot and acceleration noise, taking into account the response functions (equations 7, 8 and 9, 10). The aggregate noise spectra for each linear combination thus obtained for the $L_1 = L_2 = L_3 = L$ case are:

$$S_\alpha(f) \;=\; [4 \; sin^2(3\pi f L) + 24 \; sin^2(\pi f L)] \; S_y^{accel} + 6 \; S_y^{shot} \qquad (33)$$

$$S_\zeta(f) = 12\ sin^2(\pi f L)\ S_y^{accel} + 6\ S_y^{shot} \tag{34}$$

$$S_X(f) = [4\ sin^2(4\pi f L) + 32\ sin^2(2\pi f L)]\ S_y^{accel} + 16\ sin^2(2\pi f L)\ S_y^{shot}. \tag{35}$$

$$S_P(f) = [4\ sin^2(2\pi f L) + 32\ sin^2(\pi f L)]\ S_y^{accel} + (8\ sin^2(2\pi f L) + 8\ sin^2(\pi f L))\ S_y^{shot} \tag{36}$$

Figure 3 is a plot of these noise spectra for α, ζ, X, and P. At high frequencies, shot noise dominates. For α and ζ, the spectra of the shot noises simply add. For X, four shot noises enter, each twice and each with relative delays of zero and $2L$; thus the shot noise spectrum is modulated by $16\ sin^2(2\pi f L)$. For P, four shot noises also enter, each twice and each with relative delays of L and $2L$; thus the shot noise spectrum is modulated by $8\ sin^2(2\pi f L) + 8\ sin^2(\pi f L)$. At low frequencies, acceleration noise dominates. The factors multiplying S_y^{accel} in equations (33)-(36) follow from the definitions of α, ζ, X, and P and the acceleration noise transfer functions (equations 9, 10), under the assumptions that the (vector) acceleration noise is isotropic in the plane of LISA.

4.3. GW Sensitivity as a Function of Fourier Frequency

We take GW sensitivity to be the wave amplitude required to achieve a given signal-to-noise ratio. The sensitivity as a function of Fourier frequency was computed as $5\ \sqrt{S_i(f)\ B}$/(rms gravitational wave response for data combination i), where i is α, ζ, X, P, etc. The bandwidth, B, was taken to be 3.17×10^{-8} Hz (i.e., one cycle/year). The factor

of 5 was included because LISA sensitivities are conventionally given for SNR = 5 in a one year integration.

In Figure 4 we plot the GW sensitivity for X, assuming $L_1 = L_2 = L_3 = 10\sqrt{3}$ light seconds. This can be compared with the sensitivity curves calculated modeling LISA as a rigid, equal-arm one-bounce conventional interferometer. Schilling 1997 and Bender *et al.* 1998 envision transponders at spacecraft 2 and 3 and precisely equal arms (all of length L) for laser noise elimination. That is, they consider a transponding interferometer data combination, S:

$$y_{32} = y_{23} = 0$$

$$S = y_{21} - y_{31}$$

S has a GW signal $y_{21}^{gw} + y_{23,L}^{gw} - y_{31}^{gw} - y_{32,L}^{gw}$ composed of four pulses with times $\mu_1 l$, $\mu_2 l + L$, $\mu_3 l + L$, and $\mu_1 l + 2L$. Similarly, S has four shot noises and four acceleration noises. Our eight-pulse combination X, for the case of transponders and equal arms is, from equation (23), just $S - S_{,LL}$. That is, for this case X is just S minus a copy of S delayed by $2L$. Since every Fourier component of signal and noise in S is just multiplied by the common factor of $[1 - \exp(2\pi i f(2L))]$ to produce the corresponding Fourier component of X, the sensitivity (ratio of noise to signal) for X is exactly the same as that of S (Tinto & Armstrong 1999). Our computed sensitivity for X in Figure 4 is in very good agreement, below about 10^{-2} Hz, with an independent computation for S by Schilling 1997; in the higher frequency region our calculated sensitivity (which includes only shot noise, not beam pointing noise, etc.) is about a factor of 2 better.

Figure 5 shows the sensitivity calculation for α (β and γ sensitivities are identical) using the LISA geometry with equal arm lengths of $10\sqrt{3}$ light seconds. As with X, this

is the sensitivity averaged over source directions and polarization states. Figure 6 shows the sensitivity of ζ, both in the equilateral triangle configuration (cf. Figures 2 and 3) and for a configuration where the arm lengths are $L_2 = L_3 = 10\sqrt{2}$ light seconds and $L_1 = 20$ light seconds. Figure 7 shows the sensitivity plot for the combination P. Using the noise spectra and arm lengths above, X has the best average sensitivity ($\approx 5 \times 10^{-24}$, compared with $\approx 7 \times 10^{-24}$ for equal-arm α, $\approx 8 \times 10^{-24}$ for equal-arm P, and $\approx 1.3 \times 10^{-23}$ for equal- and unequal-arm ζ in Figure 6). In all cases, the 3dB bandwidths are comparable to the center frequencies. X and P achieve best sensitivity at lower center frequencies. α has comparable best performance, but shifted to a higher frequency. ζ has slightly worse best performance; the larger 3dB bandwidth of ζ compensates somewhat but an observer would be largely indifferent to performance of X, P, and ζ near the frequencies where ζ achieves best sensitivity.

These sensitivities and bandwidths were computed based on instrumental shot and acceleration noises only. Inclusion of expected confusion noise due to galactic binaries (Bender *et al.* 1998, Figure 1.3) would affect the low frequency band edges only, and would have little or no effect on the 3dB bandwidths and best sensitivities.

5. SUMMARY

We have given a general treatment of GW signals and the principal noise sources for an unequal arm space-borne interferometer. Our analysis was for an arbitrary gravitational wave.

By analyzing the instrument in terms of one-way Doppler shifts between pairs of spacecraft, we have derived data combinations which cancel all the laser noises while preserving the GW signals. Three of these combinations are equivalent to already-known

unequal-arm interferometers. The principal result of this paper is that there are other, previously unknown, laser-noise-canceling combinations (e.g., α, β, γ, ζ, P, Q, R) which may present advantages (e.g. in hardware design, in robustness to failures of single links, or redundancy in data analysis) for a spaceborne detector.

We presented the general GW response and the long-wavelength limits of each data combination. The rms signal response (averaged over source position and over wave polarization state) was computed for each data combination. All have the general behavior that GW response increases with increasing frequency (long-wavelength limit) until the period of the GW becomes comparable with the light-time across the apparatus. In this regime the multi-pulse signature of the GW becomes evident and the GW response as a function of Fourier frequency flattens and displays oscillations as each GW phasor adds constructively or destructively. These signal response functions were compared with noise spectra to evaluate GW sensitivity of each configuration. We used spectra of shot and acceleration noises appropriate for the proposed LISA detector, taking (as for the GW signal) explicit account of the noise transfer functions for each data combination.

ACKNOWLEDGMENTS

We thank Peter Bender and William Folkner for interesting and helpful discussions about the LISA detector. This research was performed at the Jet Propulsion Laboratory, California Institute of Technology, under contract with the National Aeronautics and Space Administration.

REFERENCES

Abramovici, A. *et al.*, Science, 256, 325

Armstrong, J. W., Estabrook, F. B., & Wahlquist, H. D. 1987, ApJ, 318, 536

Bender, P. & the LISA Study Team 1998, *Laser Interferometer Space Antenna for the Detection of Gravitational Waves, Pre-Phase A Report*, **MPQ233** (Max-Plank-Institue für Quantenoptik, Garching), July 1998

Estabrook, F. B. 1985, *GRG*, **17**, 719.

Estabrook, F. B. & Wahlquist, H. D. 1975, GRG, 6, 439

Caron, B. *et al.* 1997, Class. Quantum Grav., 14, 1461

Kawabe, K. & the TAMA collaboration 1997, Class. Quantum Grav., 14, 1477

Lück, H. & the GEO600 Team 1997, Class. Quantum Grav., 14, 1471

Schilling, R. 1997, Class. Quantum Grav., 14, 1513

Thorne, K. S. 1987, Gravitational Radiation in *300 Years of Gravitation*, S. W. Hawking & W. Israel, eds. (Cambridge University Press, pp. 330-458)

Tinto, M. 1996, Phys. Rev. D., 53, 5354

Tinto, M. 1998, Phys. Rev. D., 58, 102001

Tinto, M. & Armstrong, J. W. 1999, Phys. Rev. D. (in press)

Wahlquist, H. D. 1987, GRG, 19, 1101

This manuscript was prepared with the AAS LaTeX macros v4.0.

FIG. 1. The geometry of the 3 LISA spacecraft. Each spacecraft is equidistant from point O, with unit vectors $\hat{p}_i$ indicating directions to the three spacecraft. Unit vectors $\hat{n}_i$ point between spacecraft pairs with the indicated orientation.

FIG. 2. Root-mean-square response to gravitational waves of laser-noise-canceling combinations α, ζ, X, and P. Response has been averaged over source directions and polarization states as indicated in the text. Arm lengths: $L_1 = L_2 = L_3 = 10\sqrt{3}$ light seconds for α, ζ, X, and P (Figure 2 a,b,c,d); unequal arm ζ has arms $L_2 = L_3 = 10\sqrt{2}$ light seconds and $L_1 = 20$ light seconds (Figure 2e).

FIG. 3. Noise spectra for α, ζ, X, and P using the raw spectra of shot and acceleration noise expected for LISA combined with the noise response functions of Section 2. Arm lengths are the same as those in Figure 2.

FIG. 4. Sensitivity plot for the combination X. Arm lengths: $L_1 = L_2 = L_3 = 10\sqrt{3}$ light seconds. For this configuration, the sensitivity for X should be the same as that of a conventional equal-arm one-bounce Michelson interferometric combination, S, having the same geometry (see Section 4). Our calculated sensitivity for X, here, is in very good agreement with an independent calculation for S by Schilling 1997 for the same detector geometry (see text).

FIG. 5. As Figure 4, but for the linear combination α.

FIG. 6. As Figure 4, but for ζ, both in the equilateral triangle configuration (Figure 6a) and for an isosceles configuration where the arm lengths are $L_2 = L_3 = 10\sqrt{2}$ light seconds and $L_1 = 20$ light seconds (Figure 6b).

FIG. 7. As Figure 4, but for P in the equilateral triangle configuration.

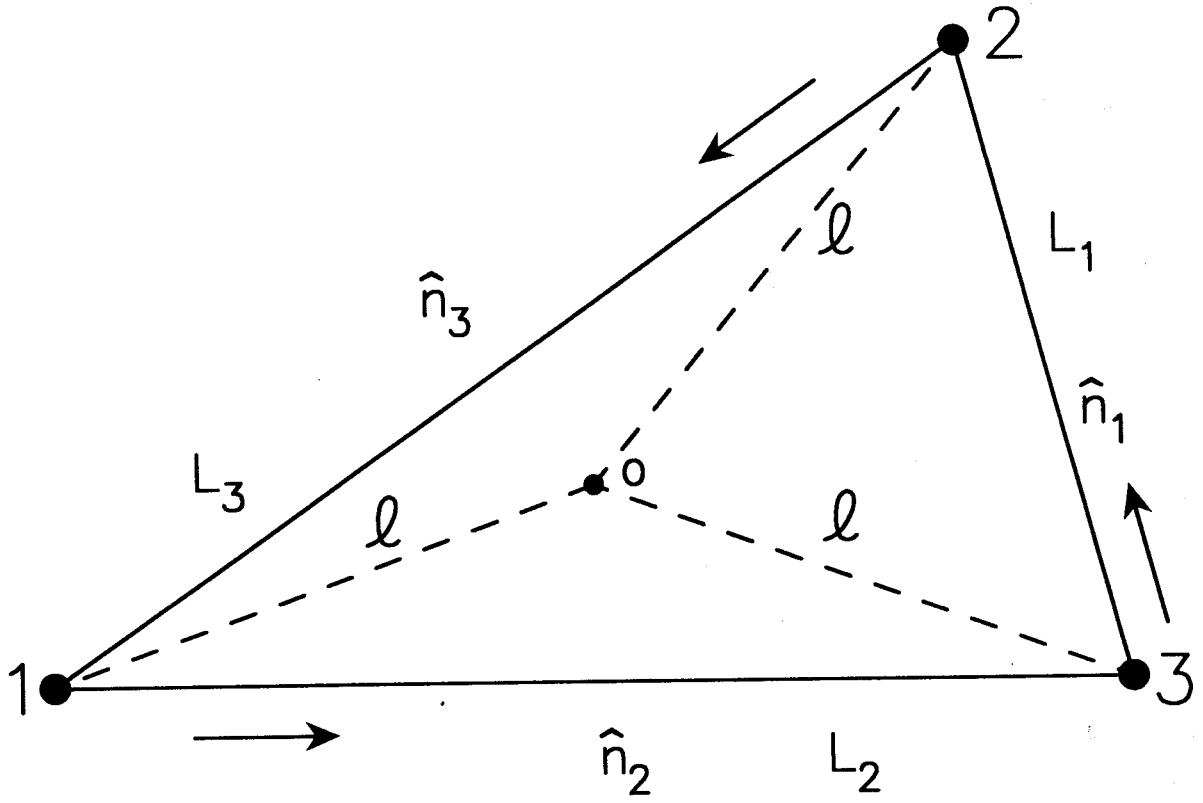
2
1
3
o
L_1
L_2
L_3
$\hat{n}_1$
$\hat{n}_2$
$\hat{n}_3$
ℓ
ℓ
ℓ

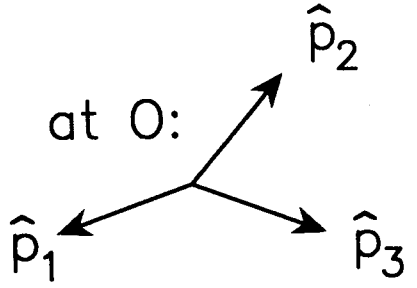
at O:
$\hat{p}_1$
$\hat{p}_2$
$\hat{p}_3$

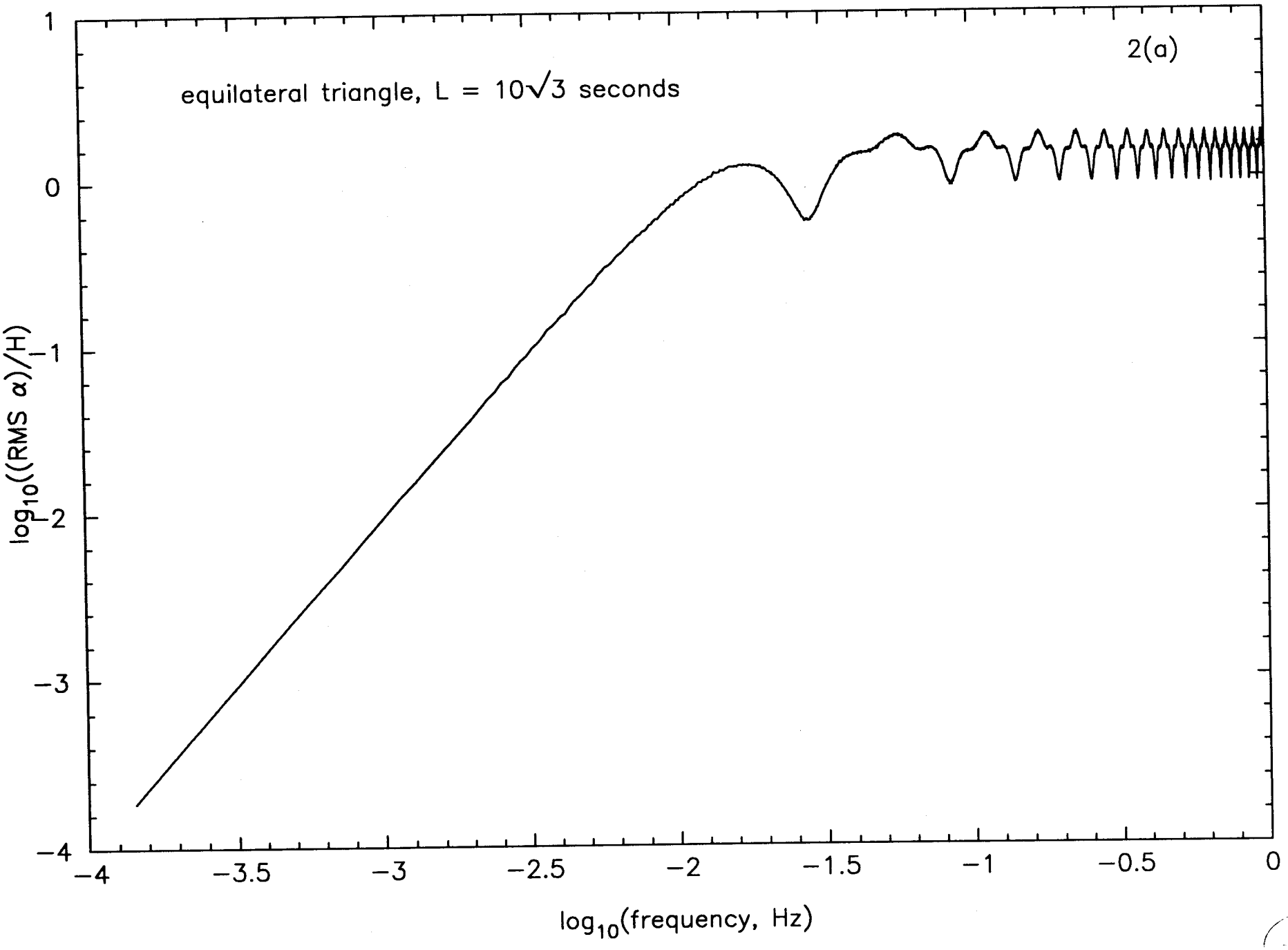
2(a)
equilateral triangle, L = 10√3 seconds
1
0
−1
−2
−3
−4
log10((RMS α)/H)
−4
−3.5
−3
−2.5
−2
−1.5
−1
−0.5
0
log10(frequency, Hz)

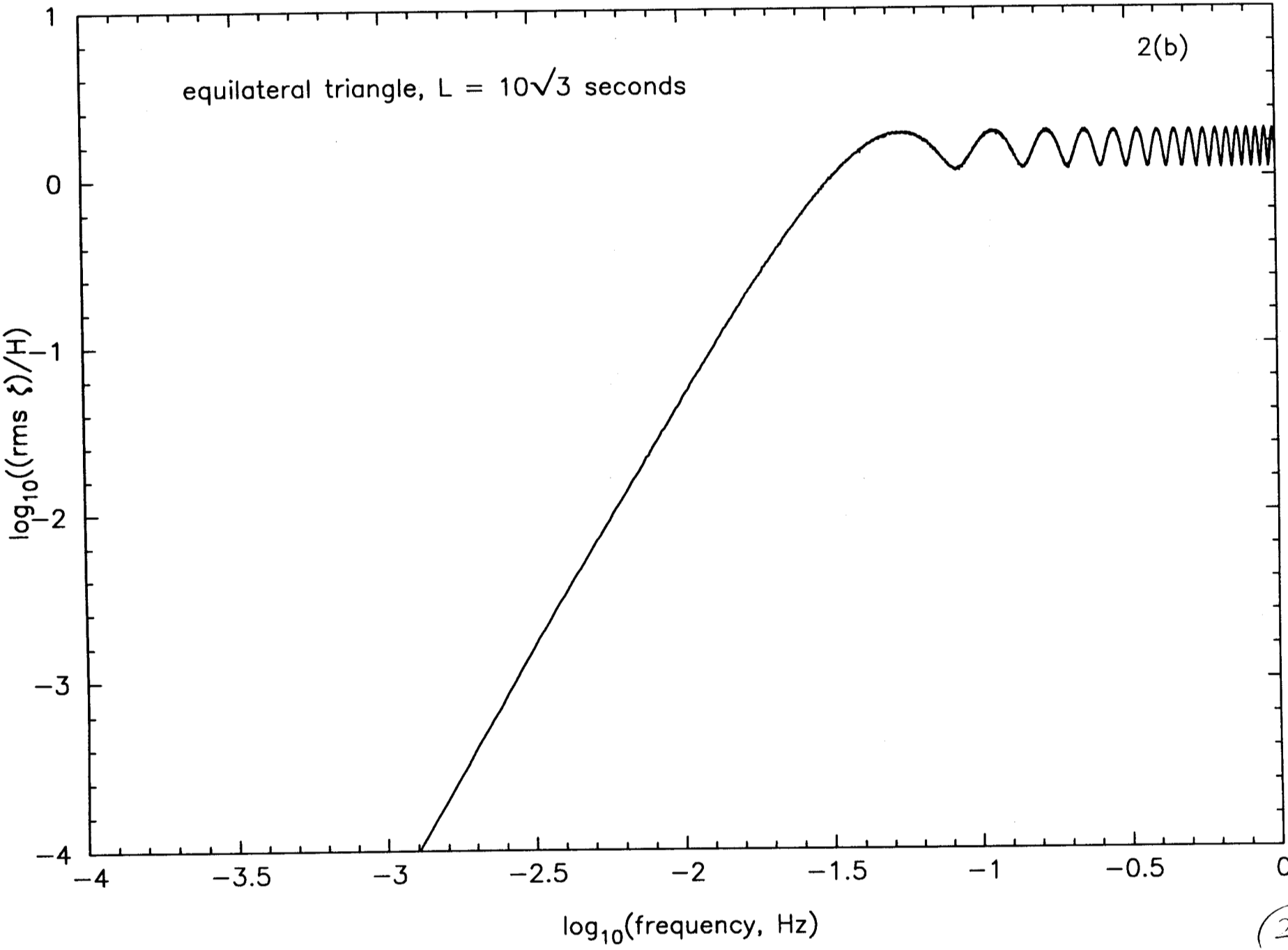
2(b)
equilateral triangle, L = 10√3 seconds
1
0
−1
−2
−3
−4
log10((rms ζ)/H)
−4
−3.5
−3
−2.5
−2
−1.5
−1
−0.5
0
log10(frequency, Hz)

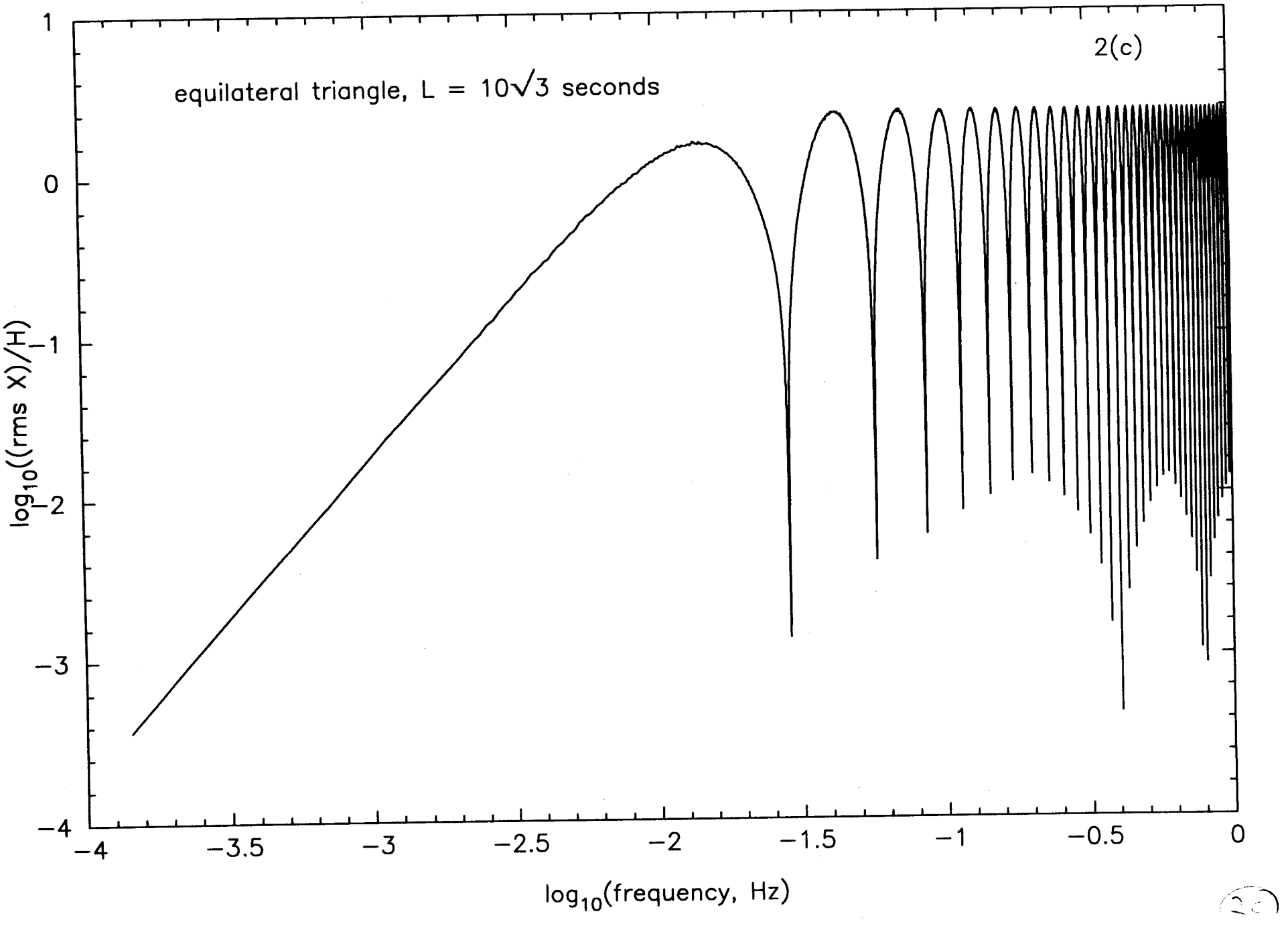
2(c)
equilateral triangle, L = 10√3 seconds
1
0
−1
−2
−3
−4
−4
−3.5
−3
−2.5
−2
−1.5
−1
−0.5
0
log10((rms X)/H)
log10(frequency, Hz)

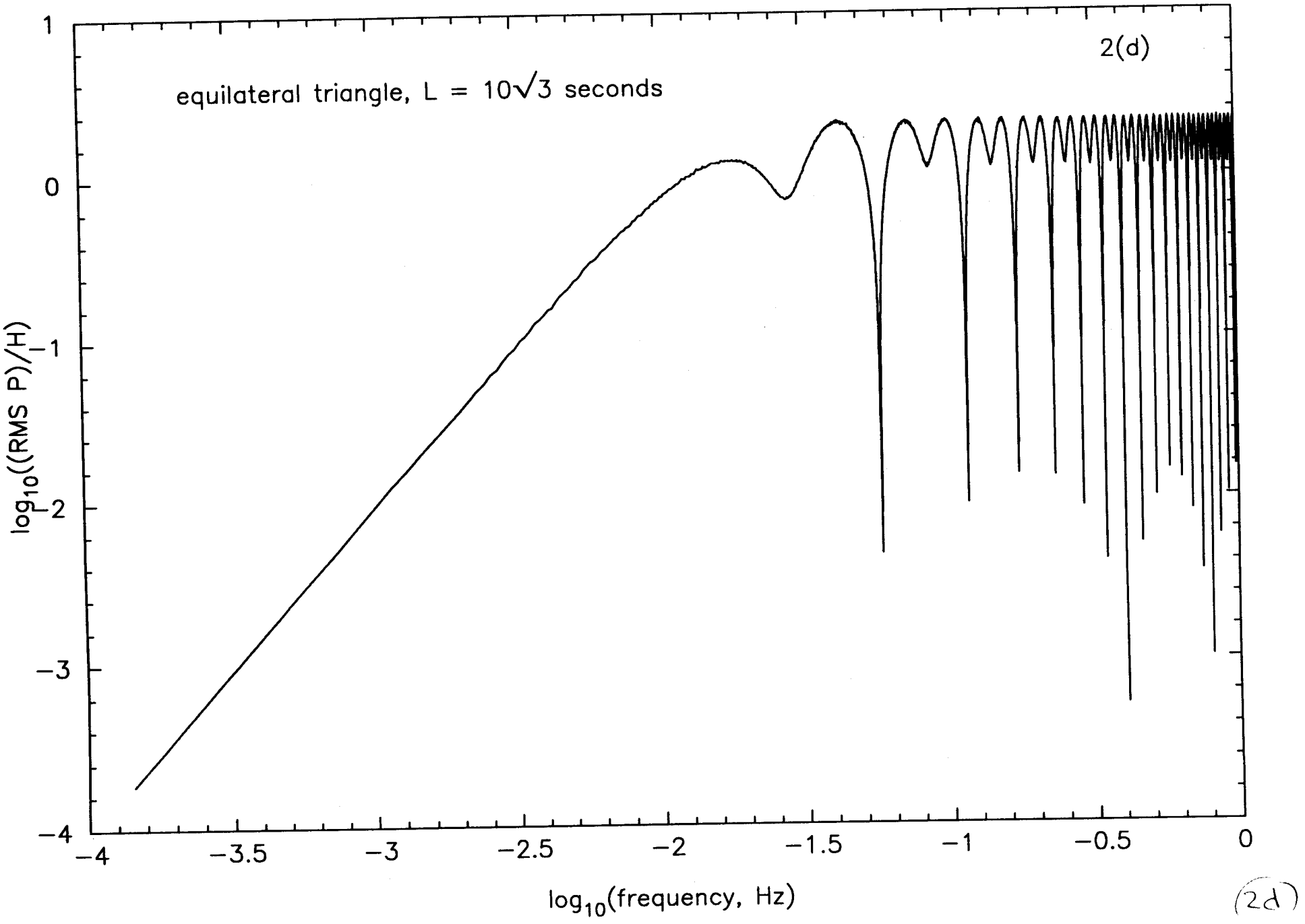
2(d)
equilateral triangle, L = 10√3 seconds
1
0
−1
−2
−3
−4
log10((RMS P)/H)
−4
−3.5
−3
−2.5
−2
−1.5
−1
−0.5
0
log10(frequency, Hz)

(2d)

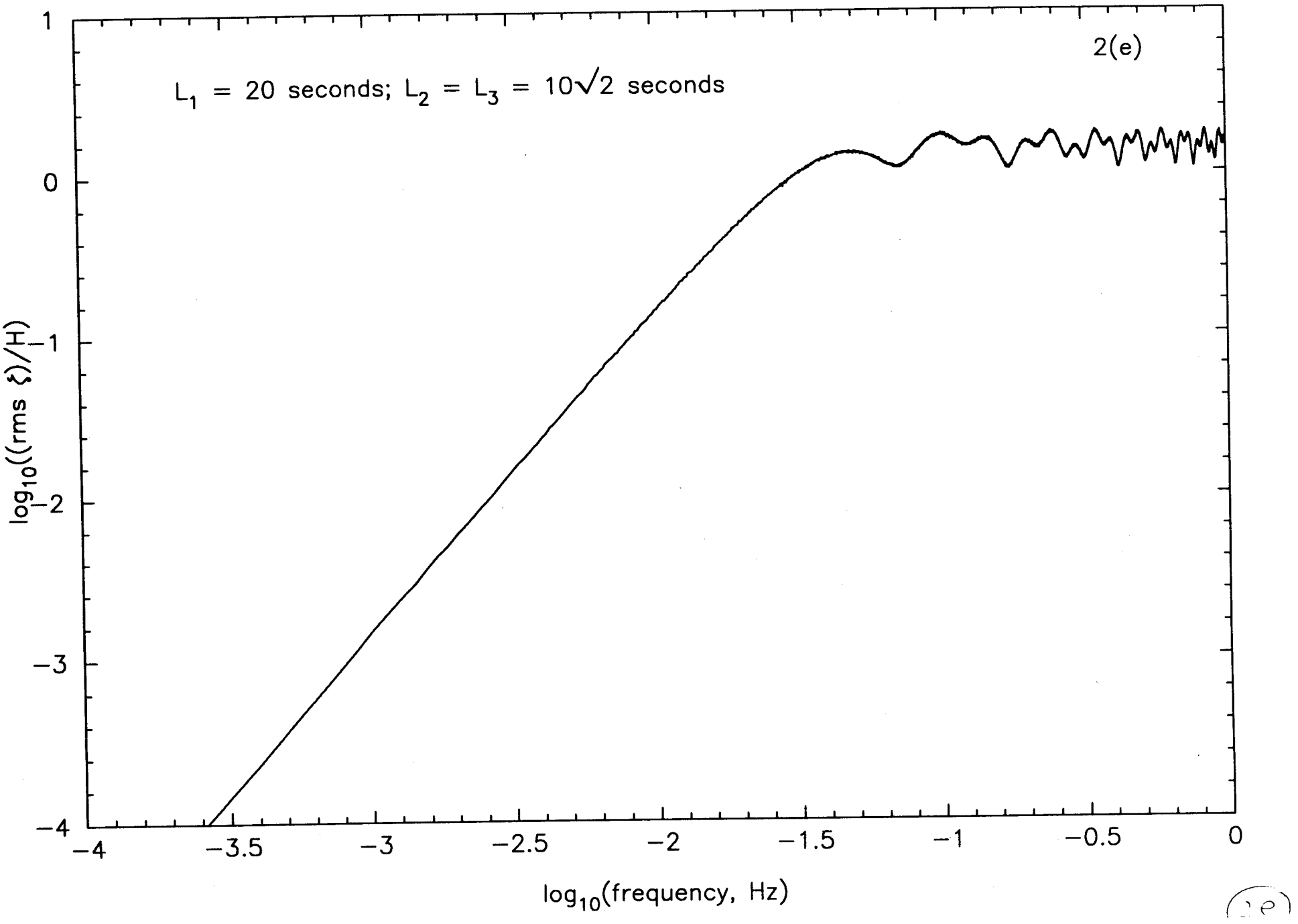
2(e)
L_1 = 20 seconds; $L_2 = L_3 = 10\sqrt{2}$ seconds
1
0
−1
−2
−3
−4
$\log_{10}((\text{rms } \zeta)/H)$
−4
−3.5
−3
−2.5
−2
−1.5
−1
−0.5
0
$\log_{10}$(frequency, Hz)

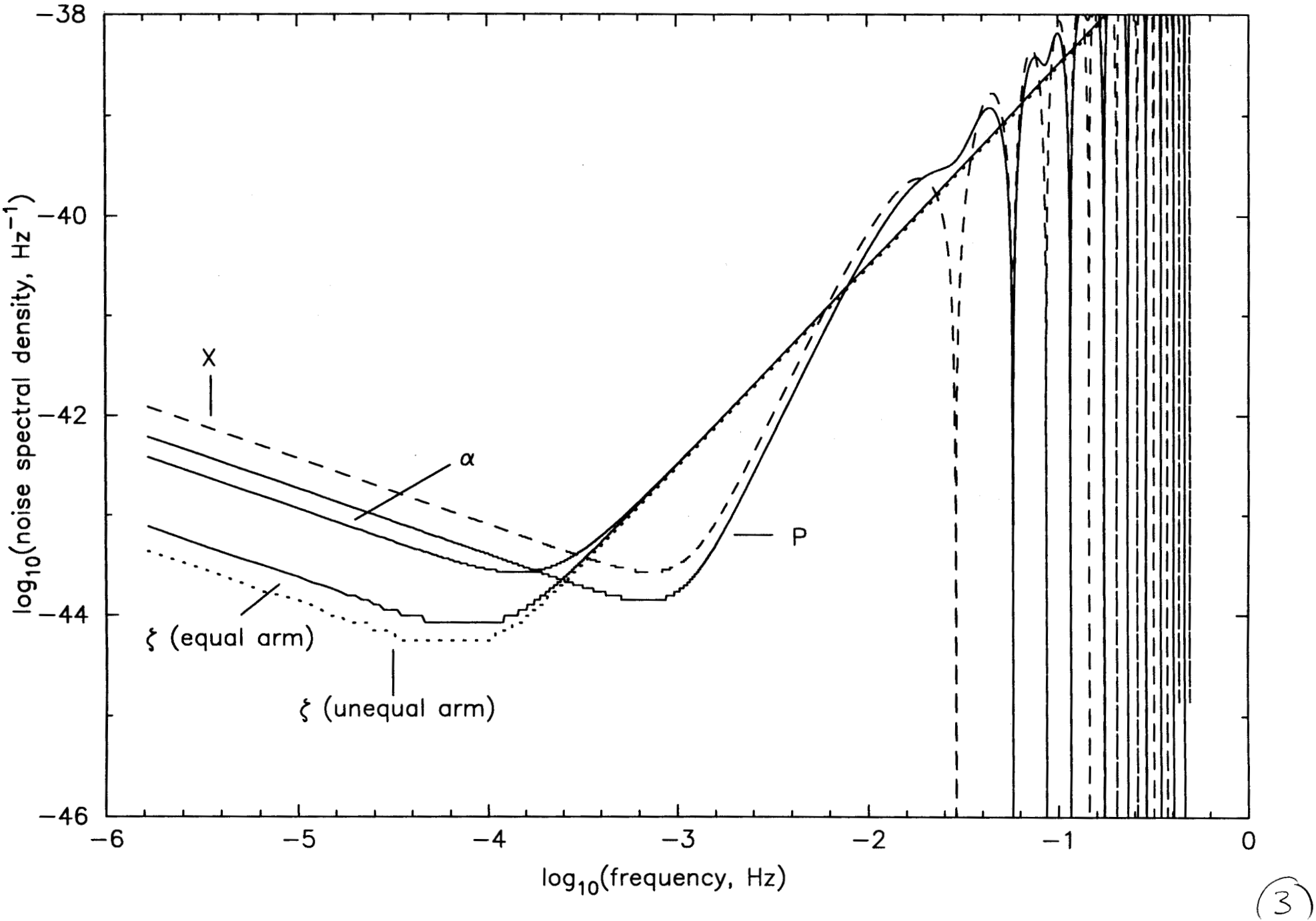
−38
−40
−42
−44
−46
−6
−5
−4
−3
−2
−1
0
log10(noise spectral density, Hz−1)
log10(frequency, Hz)
X
α
P
ζ (equal arm)
ζ (unequal arm)

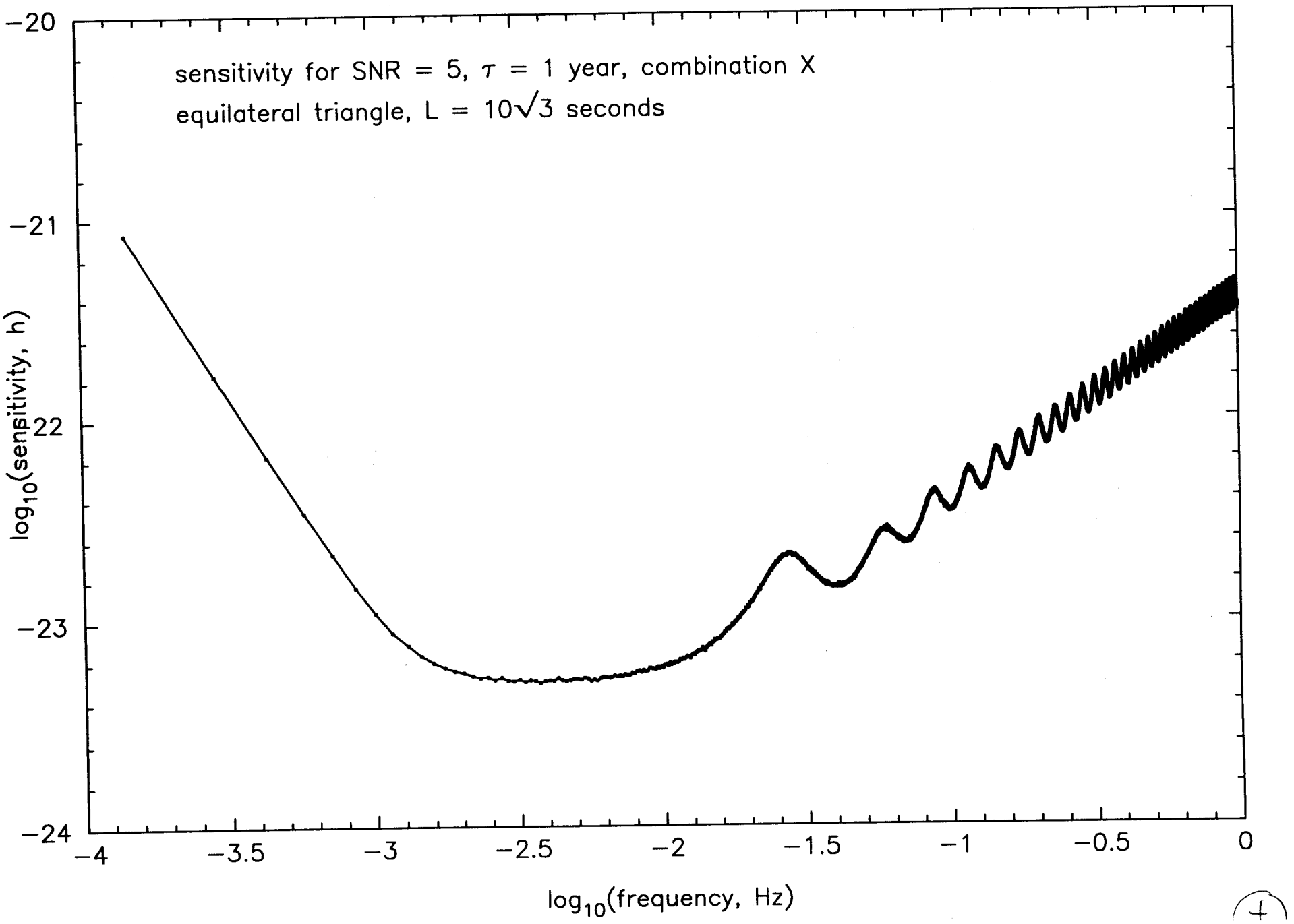
sensitivity for SNR = 5, τ = 1 year, combination X
equilateral triangle, L = 10√3 seconds
−20
−21
−22
−23
−24
log10(sensitivity, h)
−4
−3.5
−3
−2.5
−2
−1.5
−1
−0.5
0
log10(frequency, Hz)

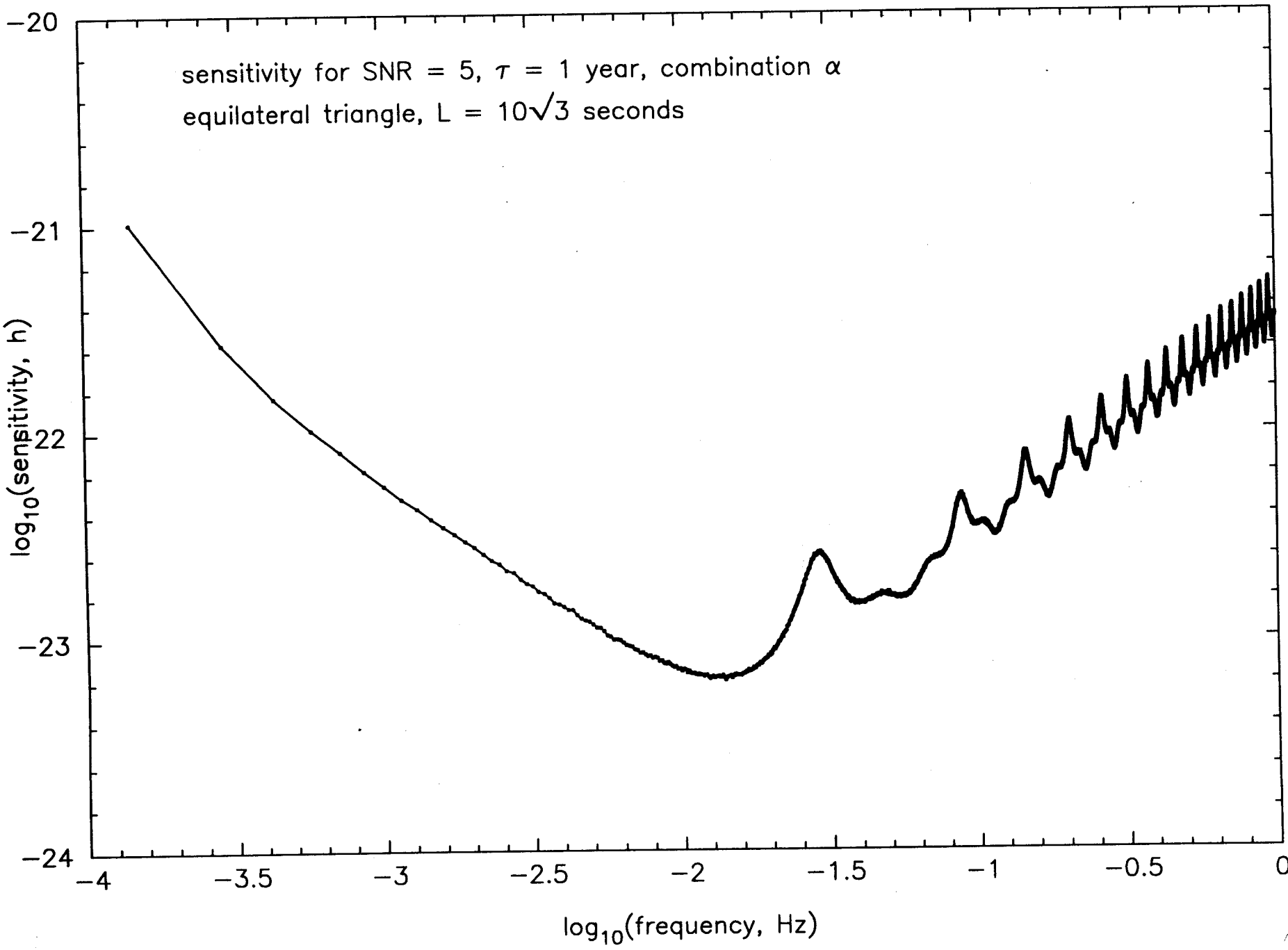
sensitivity for SNR = 5, τ = 1 year, combination α
equilateral triangle, L = 10√3 seconds
−20
−21
−22
−23
−24
log10(sensitivity, h)
−4
−3.5
−3
−2.5
−2
−1.5
−1
−0.5
0
log10(frequency, Hz)

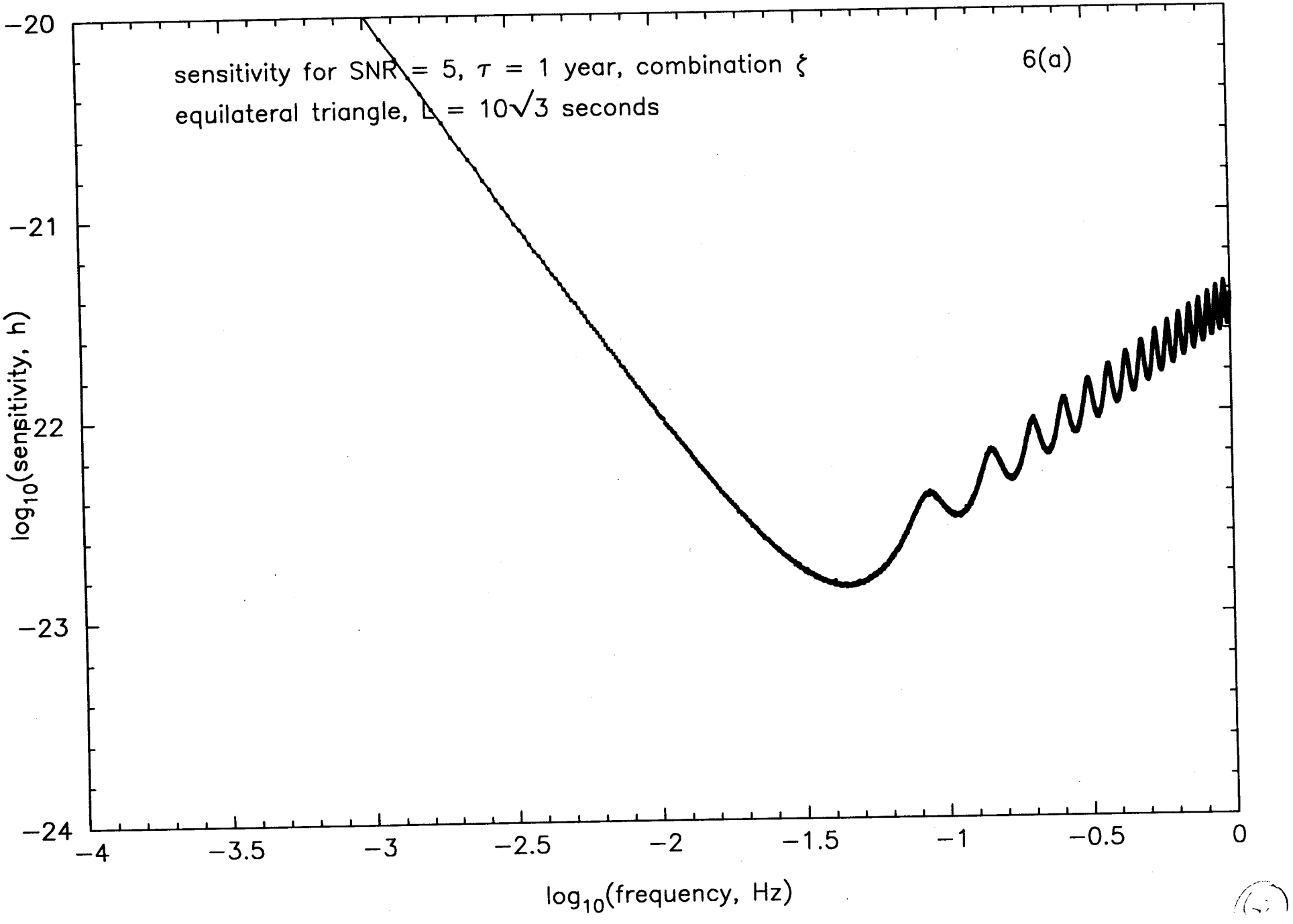
sensitivity for SNR = 5, τ = 1 year, combination ζ
equilateral triangle, L = 10√3 seconds
6(a)
−20
−21
−22
−23
−24
log10(sensitivity, h)
−4
−3.5
−3
−2.5
−2
−1.5
−1
−0.5
0
log10(frequency, Hz)

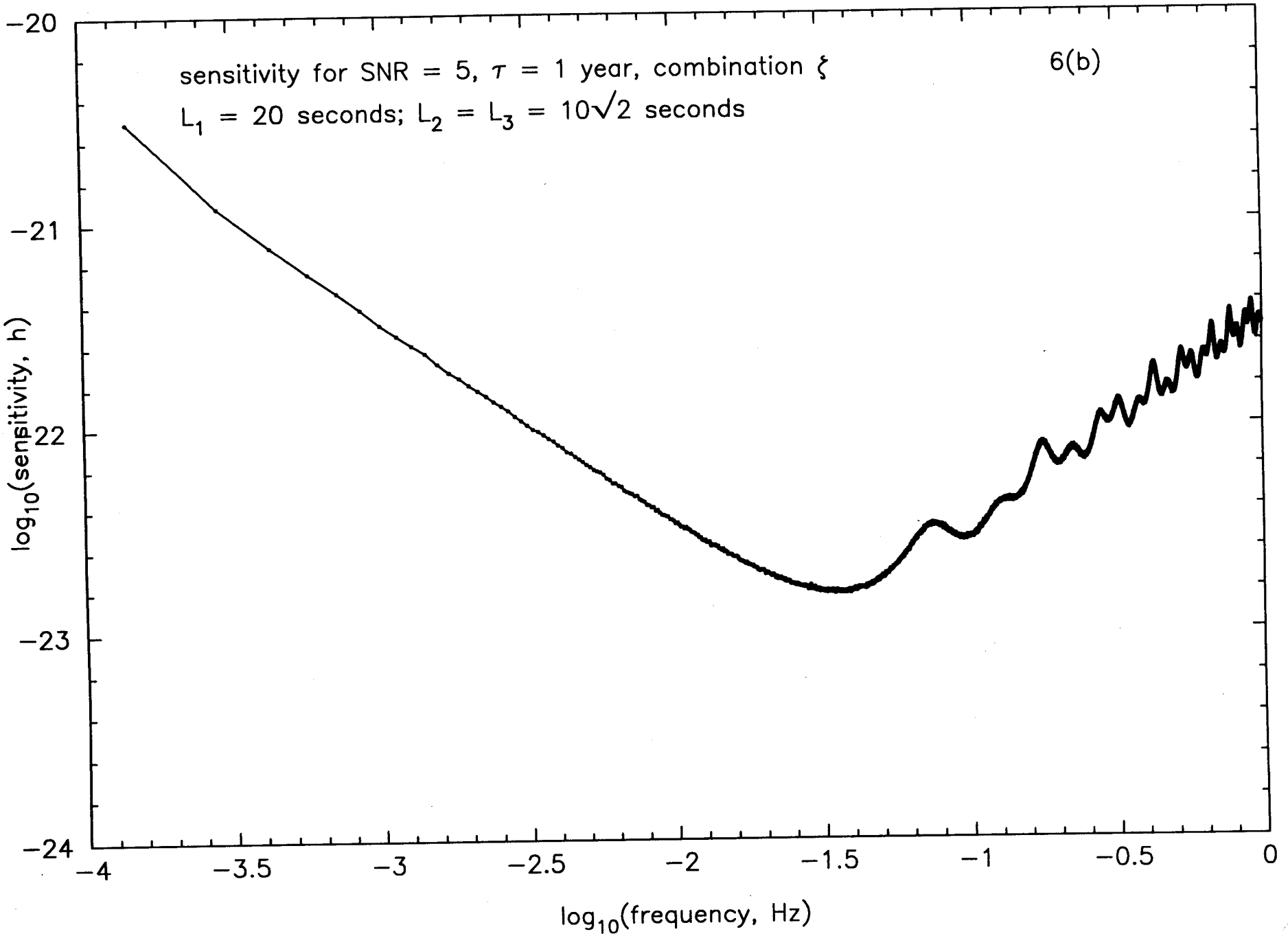
sensitivity for SNR = 5, τ = 1 year, combination ζ
L_1 = 20 seconds; $L_2 = L_3 = 10\sqrt{2}$ seconds
6(b)
−20
−21
−22
−23
−24
$\log_{10}$(sensitivity, h)
−4
−3.5
−3
−2.5
−2
−1.5
−1
−0.5
0
$\log_{10}$(frequency, Hz)

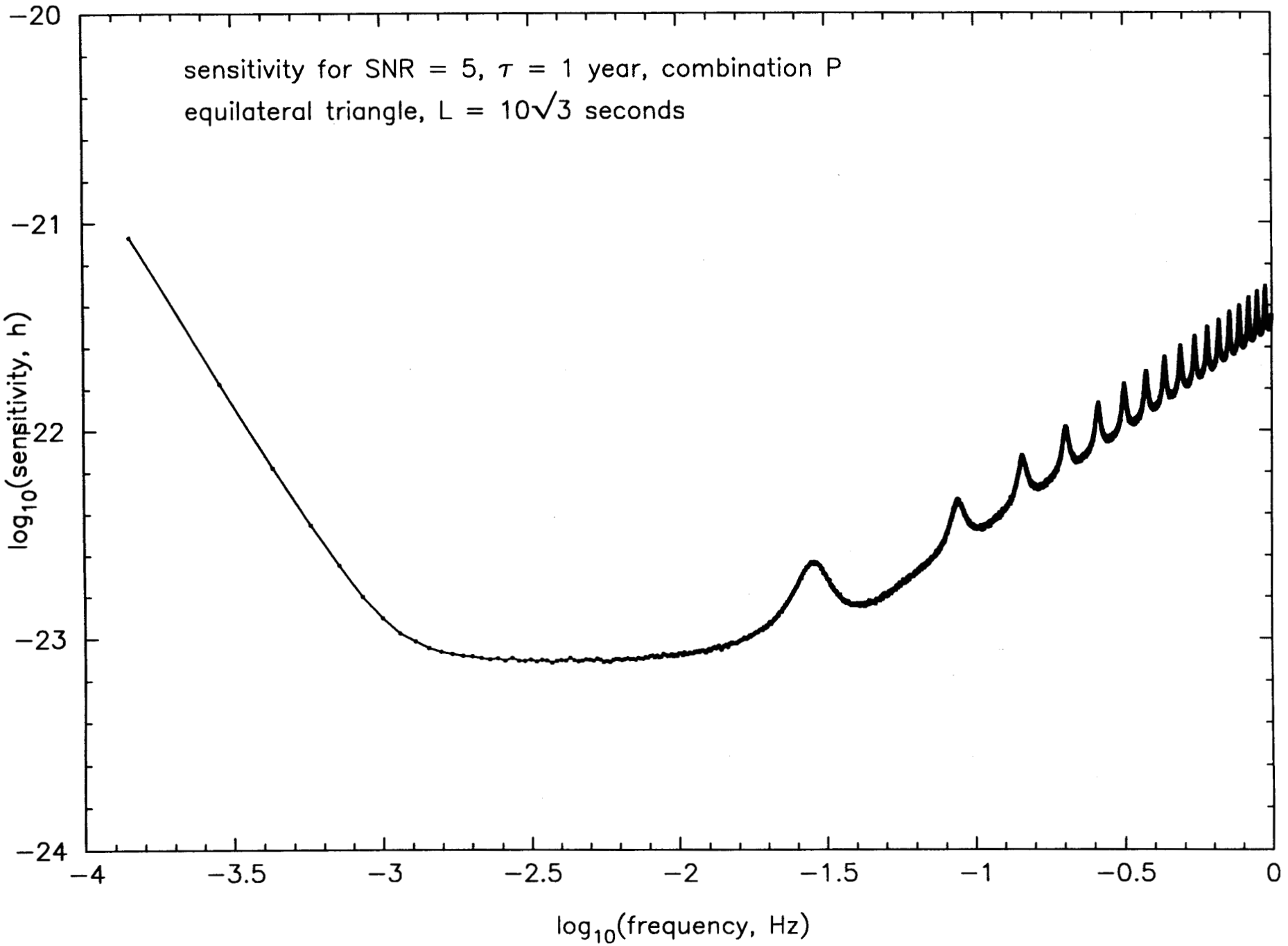
sensitivity for SNR = 5, τ = 1 year, combination P
equilateral triangle, L = 10√3 seconds
−20
−21
−22
−23
−24
log10(sensitivity, h)
−4
−3.5
−3
−2.5
−2
−1.5
−1
−0.5
0
log10(frequency, Hz)